Laser and Particle Beams (2010), *28*, 333–341.

doi:10.1017/S0263034610000285

Optimization for deuterium ion acceleration in foam targets by ultra-intense lasers

M.A. BARI,[1,2] Z.M. SHENG,[2,3] W.M. WANG,[2] Y.T. LI,[2] M. SALAHUDDIN,[1] M.H. NASIM,[1] G. SHABBIR NAZ,[1] M.A. GONDAL,[1] AND J. ZHANG[2,3]

[1]Pakistan Atomic Energy Commission, Islamabad, Pakistan
[2]Laboratory of Optical Physics, Institute of Physics, CAS, China
[3]Department of Physics, Shanghai Jiao Tong University, Shanghai, China

(RECEIVED 1 October 2009; ACCEPTED 8 April 2010)

Abstract

In this article, we investigate the effects of foam target composition and laser parameters on deuterium ion energy spectra with particle-in-cell simulations. We find that localized electrostatic fields with multi peaks around the surfaces of lamellar layers inside foam target are induced. These fields accelerate deuterium ions from thin foam layers by restricting the flow of hot electrons. This mechanism of ion acceleration called as bulk ion acceleration generates large number of high energy deuterium ions. Deuterons inside foam target are accelerated up to 126 MeV in case of oblique optimal angle of 30° where it is much greater than the normal laser incidence energy of 88 MeV.

Keywords: Bulk ion acceleration; Deuteron acceleration; Foam target; Intense laser; Laser-produced plasma

INTRODUCTION

With the achievement of laser intensities well above 10^{18} Wcm^{-2}, fast moving ions with kinetic energies approaching several tens of MeV have been observed (Clark *et al.*, 2000; Snavely *et al.*, 2000; Hatchett *et al.*, 2000). The striking features of laser-produced ions have already actuated a broad variety of studies concerning the underlying physical processes and possible applications like proton radiography (Mackinnon *et al.*, 2006), isochoric heating of matter (Patel *et al.*, 2003), and cancer therapy (Malka *et al.*, 2009). The fast ignition concept pertaining to inertial confinement fusion (ICF) also enhances interests in laser-driven ion acceleration (Tabak *et al.*, 1994; Roth *et al.*, 2001; Eliezer *et al.*, 2007; Hora, 2007; Winterberg, 2008; Naumova *et al.*, 2009).

In the interaction of femtosecond laser pulses with solids electron beams are generated and accelerated to highly relativistic energies. The laser pondermotive force pushes these hot electrons out of the laser focus. The expelled electrons form an electric field at target front surface due to charge separation of electrons and ions. Ions produced at the front surface are accelerated inside the target. This mechanism of ion acceleration is called front side acceleration. Fast electrons also propagate away from laser irradiated surface toward the vacuum forming an electrostatic sheath which results in ion acceleration in front of the target (Temporal *et al.*, 2002). A significant number of laser-driven hot electrons propagate through the target and emerge from target rear surface. Space-charge separation at target rear surface forms an electrostatic filed sufficient for ionizing atoms and causes strong acceleration of ions along the target normal. This mechanism of ion acceleration is called Target Normal Sheath Acceleration (TNSA) (Wilks *et al.*, 2001; Brambrink *et al.*, 2006; Limpouch *et al.*, 2008). At moderate laser intensities, a collisionless electrostatic shock wave is formed in thin foils, which can accelerate ions to high energy (Chen *et al.*, 2007; Liu *et al.*, 2009). This mechanism of ion acceleration exists widely in space and astrophysical plasmas. At high laser intensities ($\sim 10^{21}$ watt/cm^2), the ions can be accelerated to high energies due to radiation pressure acceleration (Yin *et al.*, 2006, 2007; Lifshitz *et al.*, 2006; Roth *et al.*, 2005). Recently, radiation pressure acceleration mechanism has been shown by circularly polarized laser pulse interacting with a double layer target (Bin *et al.*, 2009). In radiation pressure acceleration, the laser energy is transferred directly and efficiently to fast ions and monoenergetic ion beams are generated.

Combination of several-micron targets in a periodic structure just like the low density foam target was proposed to enhance the laser energy conversion from laser pulse to

Address correspondence and reprint requests to: M. Abbas Bari, Pakistan Atomic Energy Commission, P. O. Box 1114, Islamabad, 44000, Pakistan. E-mail: kmabari@gmail.com

proton beam (Gibbon and Rosmej, 2007; Andreev *et al.*, 2009). It led to an increase in local concentrations of fast electrons, which in turn generate high energy ions. Enhancement in laser energy absorption from a nanostructure target consisting of large number of nanoscale-size components has been studied by a number of authors (Kulcsár *et al.*, 2000; Rajeev *et al.*, 2003; Fournier *et al.*, 2004; Sumeruk *et al.*, 2007; Bagchi *et al.*, 2008). Increasing the number of small targets could improve the conversion efficiency of laser energy to ion beam energy (ter-Avetisyan *et al.*, 2008; Andreev *et al.*, 2009). In such targets, the internal acceleration of ions is caused by the electric fields localized near target surface. We believe that this mechanism for field generation in foam target is similar to those with other structured targets but just with different size and geometry.

The aim of the present work is to investigate another kind of ion acceleration mechanism called bulk ion acceleration (Zhang *et al.*, 2005; Li *et al.*, 2005). The interest of this investigation stems from the fact that the energy spectrum of ions and mechanisms of ion acceleration from foam targets are very sensitive to foam composition and foam microstructure. Second, interaction of laser light with low density foam is of great importance for ICF applications (Borisenko *et al.*, 2008). Low density foam (1–100 mg/cm^3) is used as a component of ICF target in direct drive scheme. It provides uniform laser energy absorption as well as the suppression of high-Z plasma expansion in ICF (Mulser *et al.*, 2005; Hoffmann *et al.*, 2005; Jungwirth, 2005; Hora, 2007) plasmas. It is necessary to investigate the laser light interaction with low density foam and particle transport inside the irradiated samples.

We investigate here how the foam density in a foam target irradiated by ultra-intense laser pulse affects the features of deuterium ion acceleration. We used a foam target consisting of regular micro-thin layers. Thickness of the thin layers is around a micron and separation gap between neighboring layers is on the order of a few microns. Hot electrons produced and transported in the target, generate localized electrostatic fields having multi-peaks around the surfaces of thin layers inside the target. These fields inhibit hot electron transport and meanwhile accelerate ions inside foams and forming a bulk ion acceleration in contrast to the surface acceleration at the front and rear sides of a thin solid target. The number of accelerated deuterons could be significantly enhanced in bulk ion acceleration. Our numerical simulations show that the deuterons energy reaches its value of 126 MeV at an oblique angle of 30° and 88 MeV at normal incidence. This mechanism of ion acceleration may be beneficial for applications like laser-driven neutron sources, short lived isotope production, and fast ignition by fast protons.

PARTICLE-IN-CELL SIMULATIONS OF LASER-FOAM INTERACTIONS

We have performed one-dimensional (1D) and two-dimensional (2D) fully relativistic particle-in-cell (PIC simulations in order to understand the physical processes underlying in bulk ion acceleration. A foam target is composed of irregular lamellar layers distributed randomly in a three-dimensional (3D) geometry. In 1D-PIC simulations, foam is an array of thin solid films with a gap between neighboring layers. The advantage with 1D foam is its simplicity in understanding the main physics involved in this study.

Plasma density in pre-plasma region increases exponentially from $0.1n_c$ to about $1n_c$ in a scale length of $40\lambda_L$ (see Fig. 1a), where n_c is the critical density and λ_L is the laser wavelength. The pre-pulses and amplified spontaneous emission at the leading edge of a high power laser pulse produce the pre-plasma, which can play a significant role in defining the properties of the ion beam. A moderate laser contrast such as 10^{-7} is suitable to create pre-plasma in-front of the foam target. The pre-plasma in-front of the foam target does not eliminate the vacuum-plasma surface inside the foam target. The high density region consists of 40 thin layers of plasma with density $40n_c$. Thickness of each layer is $d = 0.2\lambda_L$, and void or separation gap between neighboring layers is $L = 4\lambda_L$. The target consists of fully ionized deuterons (ion mass is $3672m_e$), D^+ and carbon ions with an ionization of 4, C^{+4}. The laser pulse with dimensionless amplitude $a = eE_0 = eE_0/m_e\omega_L c = 30$ is incident normally and obliquely on foam target as well. The laser pulse of duration 300 laser cycles has a sine-square profile. The simulation box is 500 λ_L along the x-axis. For large ion density, we keep 40 number of lamellar foam layers constant.

Figure 1b shows the induced longitudinal electric fields and electron density distribution for foam target at $t = 400$ laser cycles. When laser pulse interacts with foam target, hot electrons produced in the laser-plasma interaction are transported inside the foam. An electrostatic field with multi-peaks is built-up around each lamellar layer inside the foam, as shown in Figures 1b and 1d. It is expected that this multi-peaked field accelerates ions to high energies. Figure 1c indicates that the density of deuterons at two different times $t =$ 300 and $t = 500$. At time $t = 300$, most of deuterons are still present at their position of emission. But at a later laser period, i.e., at $t = 500$, almost all of deuterons are pushed away from their emitting foam layers. As the electrostatic field induced around each lamellar layer appears to be ambipolar, so deuterons at the two sides are accelerated in opposite directions. The return electron current around each lamellar layers is the partial reason of this ambipolar field structure.

Electrons traveling through voids or gaps in the foam structure are not neutralized by ions, which remain in the high density regions called threads, and set-up localized electrostatic fields. The localized electrostatic fields formed inside the foam target accelerate ions from thin foam layers by restricting the flow of hot electrons. Flow of electrons is inhibited from traveling through the foam due to high density threads and voids making up the foam structure. The filamentation of hot electron beam inside foam target has been observed possibly due to electromagnetic

https://doi.org/10.1017/S0263034610000285 Published online by Cambridge University Press

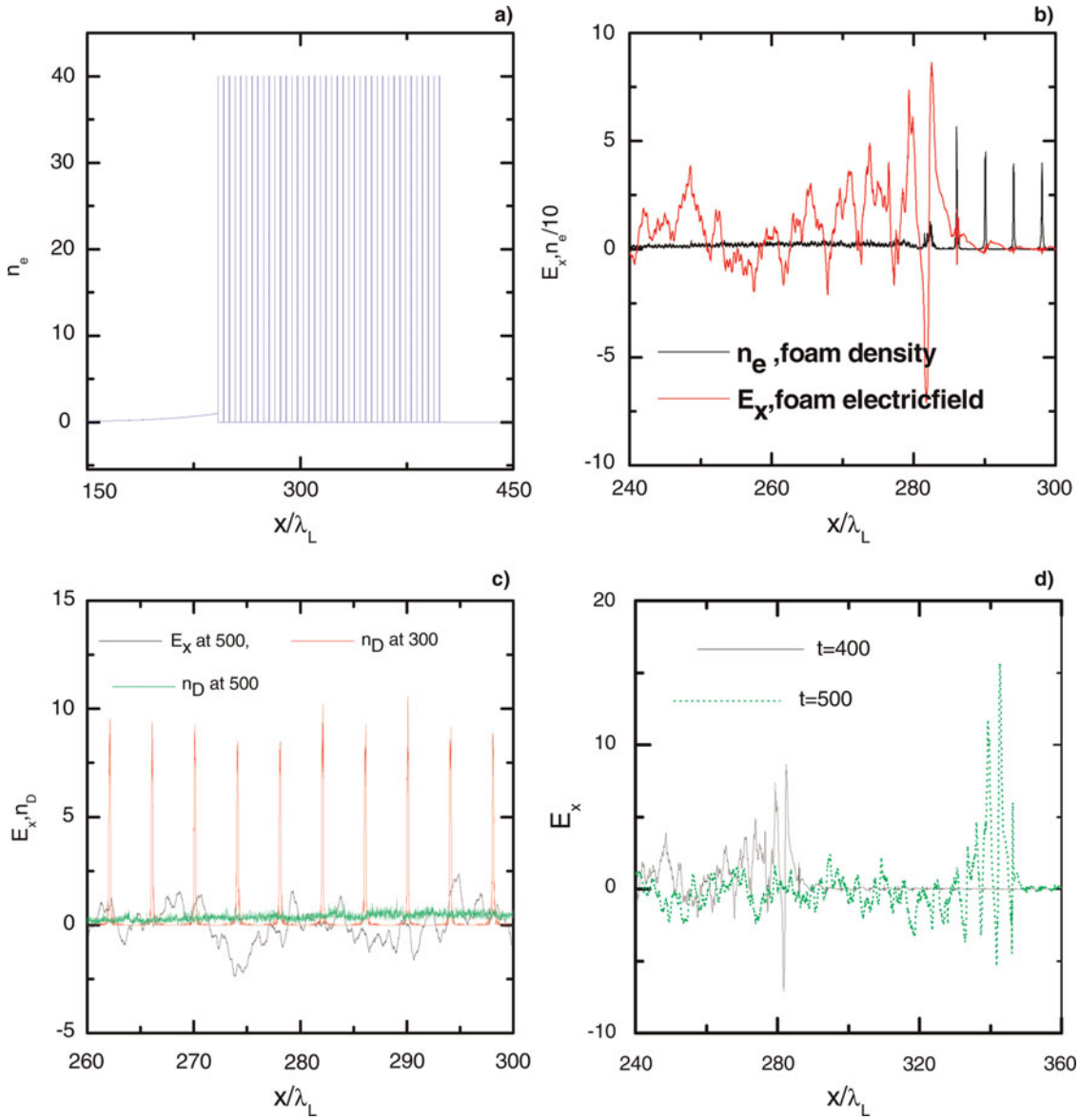

Fig. 1. (Color online) The *p*-polarized light is normally incident on the foam target. (**a**) Initial electron density distribution used in the 1D-PIC simulations. (**b**) Induced electric fields inside the foam targets and electron density at $t = 400$ laser cycles. (**c**) The deuteron densities inside the foam target at $t = 300$ and $t = 500$, and the longitudinal electric field at $t = 500$. Longitudinal electric fields at $t = 400$ and 500 laser cycles.

instabilities of the Weible type (Jung *et al.*, 2005; Ramakrishna *et al.*, 2009). When hot electron current exceeds the Alfvén limit, the magnetic field associated with the beam will affect the electron trajectories back and will restrict their movement in the forward direction.

The inhibition to the propagation of fast electrons in plastic foams is due to resistive electric fields (Batani *et al.*, 2002). As the fast electron beam passes through a target, a return current must be set-up to maintain the quasi-neutrality or the fast electron beam will be unable to propagate. At lower plasma densities, such as those found in foam targets, there are fewer background electrons to supply the return current and therefore a larger inhibition to the fast electrons is expected.

Figure 2 shows the ion distributions in the longitudinal phase. Bulk ion acceleration is found inside the foam target (see Fig. 2a). It is caused by the induced field around the surfaces of each lamellar layer. Figure 2b is an evidence for bulk ion acceleration region, which clearly shows the acceleration of almost all ions. In our simulations, C^{4+} is also accelerated to a similar level of the acceleration of deuterons, as shown in Figure 2c. We consider the similar charge to mass ratios for our ionized deuterons and carbon ions. The energy distribution of deuterons is plotted in Figure 2d. It conveys the information of bulk ion acceleration inside the foam.

Ion acceleration from different foam targets was found to be very sensitive to laser and target parameters (Okihara

https://doi.org/10.1017/S0263034610000285 Published online by Cambridge University Press

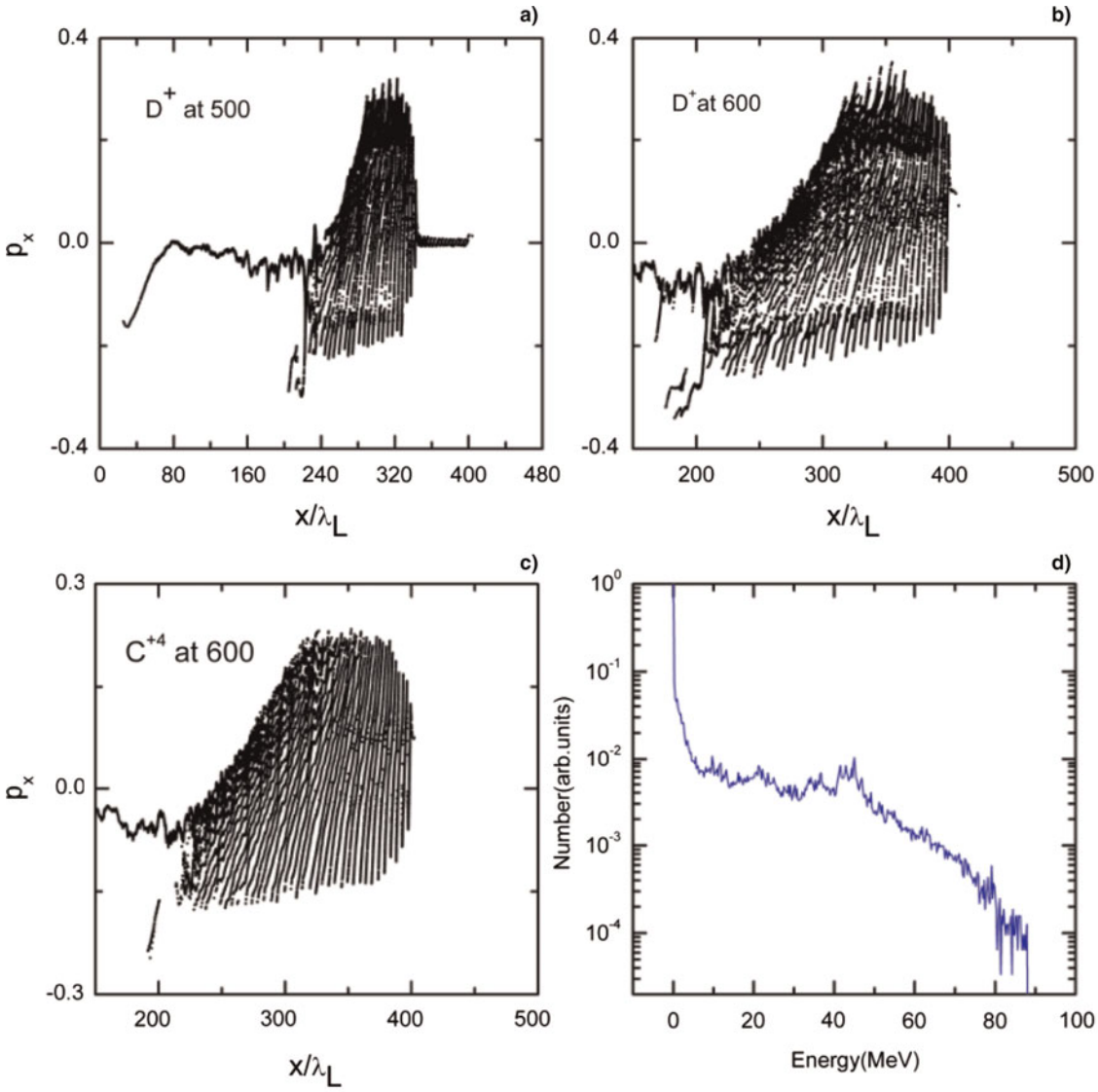

Fig. 2. (Color online) The longitudinal momenta of deuteron ions at $t = 500$ laser cycles (**a**), (**b**), and (**c**) are the close-up illustrations for the deuterium and carbon ion acceleration inside the foam target at $t = 600$. (**d**) Energy distributions of deuteron ions at $t = 500$ laser cycles.

et al., 2004; Li *et al.*, 2005; Willingale, 2007). Different foam target composition and structure, i.e., the void gap and layer thickness can come up with different mechanisms of ion acceleration. For large voids of the order of 10 μm (Okihara *et al.*, 2004), ions acceleration inside the foam target is due to Coulomb explosion. In another experimental study, foam targets of various densities with gap size and layer thickness in the sub-micron range were used (Willingale, 2007). Protons from such low density foam targets are accelerated by the mechanism of TNSA. Protons at the back of these targets were accelerated up to 30 MeV.

Our new results and previous findings show that ion energy and mechanisms of ion acceleration from foam target depends significantly on foam parameters, i.e., the thickness "*d*" and separation length or gap size "*L*" between neighboring foam layers. Figure 3 presents a comparison of the deuteron energy distributions for different foam parameters. At a given foam density ($40n_c$) and foam thickness ($d = 0.2\lambda_L$), a larger separation "*L*," can result in a higher deuteron energy because the deuterons have a long acceleration distance. Figures 3a and 3b show that the deuteron energy increases with the separation gap. The foam densities used in Willingale (2007) and in our simulations are almost the same. If the separation length and layer thickness are in the sub-micron region, the laser at given intensity cannot propagate completely throughout the target and the foam target behaves as a solid target. Ions are accelerated at rear surface of the target due to TNSA mechanism. For too large separation gap (Okihara *et al.*, 2004), the Coulomb explosion from micro structures inside the foam may appear due to the weak induced fields along large gap size. Therefore, by tailoring the distance between

https://doi.org/10.1017/S0263034610000285 Published online by Cambridge University Press

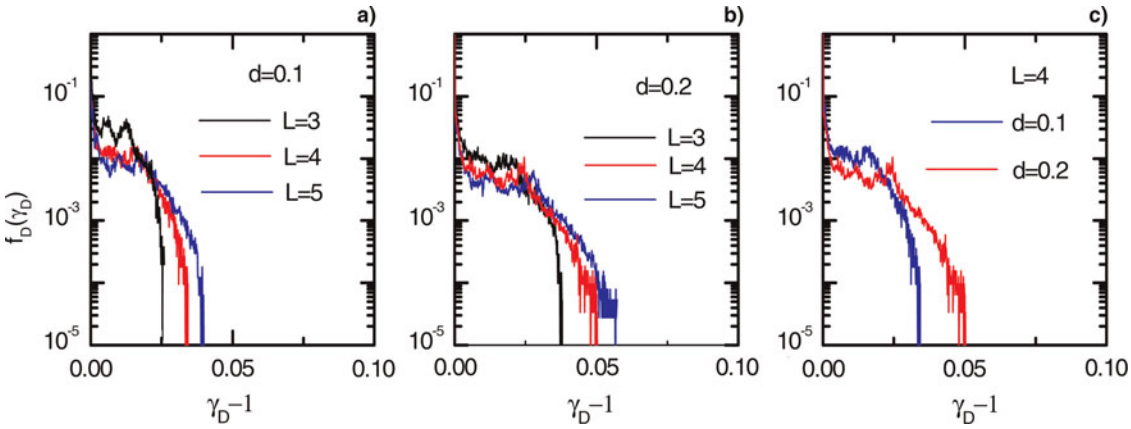

Fig. 3. (Color online) (**a**), (**b**), and (**c**) are energy distributions of deuterons at $t = 500$ for different foam target parameters and γ_D is the Lorentz factor for deuterons.

adjacent layers and layer thickness, ion energy can be enhanced to large extent. To our knowledge, no study of ion acceleration from foam targets reported large densities of ions due to bulk acceleration. The optimal density of the foam is the one where separation gap and thickness are suitable for bulk ion acceleration. Deuterons energy remains almost 88 MeV beyond the optimized peak density of $40n_c$ like $50n_c$ or $60n_c$ but ion density is much reduced as the laser energy cannot propagate to higher depths inside foam target. The bulk ion acceleration becomes less effective at higher foam densities.

OPTIMIZED LASER PARAMETERS

We find that deuterium ion energy can be increased further by oblique incidence of the laser pulse on foam target. We optimized the incidence angle of the laser pulse on the foam target with 1D-PIC simulations. The energy transfer from *p*-polarized obliquely incident electromagnetic wave to the electrons depends on the incidence angle. The ion beam energy from a double layer target is substantially higher than the normal incidence due to strong electron heating *via* vacuum heating (Morita *et al.*, 2008). Strong electron heating results in strong electric field generation which in turn leads to more efficient ion acceleration.

Figures 4c and d shows that deuterium ions have maximum energy of 126 MeV for an incidence angle of 30° and 88 MeV at normal incidence of the laser pulse. Figure 4b shows that the transfer of laser energy to electrons is more efficient at an optimized angle of 30°. For the oblique incidence, electrons are accelerated to higher energy or a higher temperature because of the formation of the electron plasma oscillations. Excitation of such electron plasma oscillations in the interaction of obliquely *p*-polarized relativistically strong electromagnetic wave with non-uniform plasma has been studied in Bulanov *et al.* (1994). The breaking of the plasma wave occurs either because of the non-uniformaity of the ion density distribution at the boundary of the plasma near the end of pre-plasma, or to the increase of the wave vector of the plasma wave. Breaking of the plasma wave occurs and leads to the heating of the electrons to higher velocities many times higher their quiver energy. As a result, electrons can propagate a longer distance before they are stopped by the electrostatic fields established around the surface of the individual thin plasma layers. The bulk acceleration appears more effective due to electrostatic fields produced to a greater depth inside the foam target (see Figs. 4b and 4d). Figures 4c and 4d show the energy distribution of deuterium ions for the oblique and normal incidence of the laser pulse. By comparing Figures 4d and 5, we see that deuterium ions have almost the same energy in case of oblique laser incidence and high intensity laser ($a = 60$). The deuterium ion acceleration for the optimized angle appears more efficient than for normal incidence of the high intensity laser. Finally, we simulate the results for deuterium bulk ion acceleration as a function of laser intensity, as shown in Figure 5. The deuterium ion energy increases with laser intensity as more intense laser has the ability to generate more intense electrostatic fields inside the foam target. It is however of great interest to study the interaction of a relativistically strong electromagnetic wave in overdense plasma and the corresponding acceleration of electrons, ions and generation of high harmonics.

We have confirmed the underlying physics involved in our 1D-PIC simulations by performing 2D-PIC simulations. Figure 6a shows our model for the 2D-PIC simulations and adopts the similar simplified regular distribution for the lamellar foam structure. All of the laser and plasma parameters in 2D-PIC simulations are the same as in the 1D case. We consider a linearly polarized laser pulse normally (see Figs. 6a and b) and obliquely incident on the target. The laser pulse arrives at the mass plasma after 10 laser cycles. The total simulation domain is $160\lambda_L \times 10\lambda_L$ and the total number of electrons and ions in the simulation box are 5×10^6 each. The pre-plasma length is $4\lambda_L$ and the foam plasma size is $36\lambda_L$. We simulated the oblique incidence of the laser pulse by taking the oblique plasma, as shown in Figure 6b. We found that the physical processes

https://doi.org/10.1017/S0263034610000285 Published online by Cambridge University Press

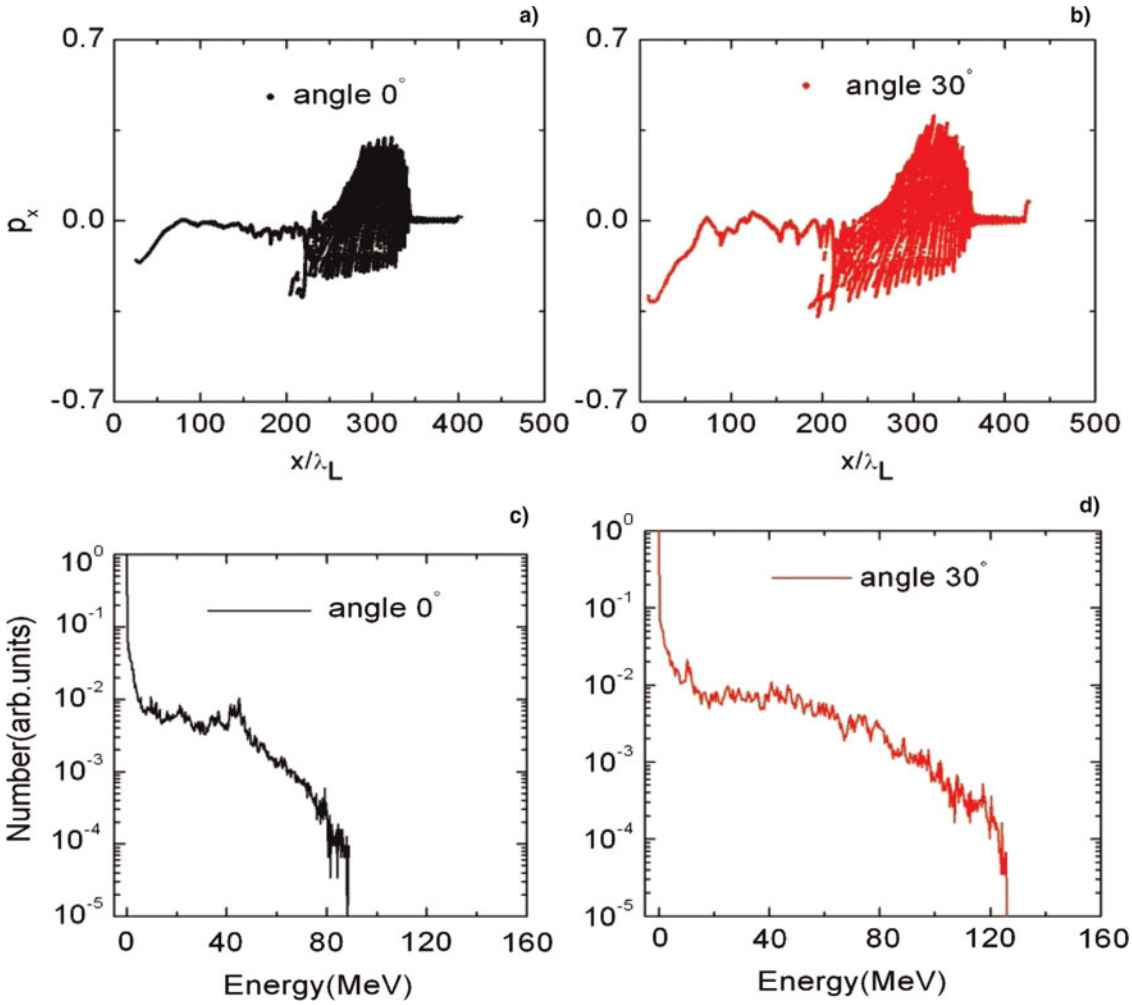

Fig. 4. (Color online) A schematic view of *p*-polarized light obliquely incident to the plasma gradient. Longitudinal momentum of deuteron ions at $t = 500$ laser cycles for a normal incidence (**a**). (**b**) For oblique incidence of the laser pulse at $t = 500$ laser cycles. (**c**) and (**d**) are the corresponding energy distributions of deuteron ions at $t = 500$ laser cycles.

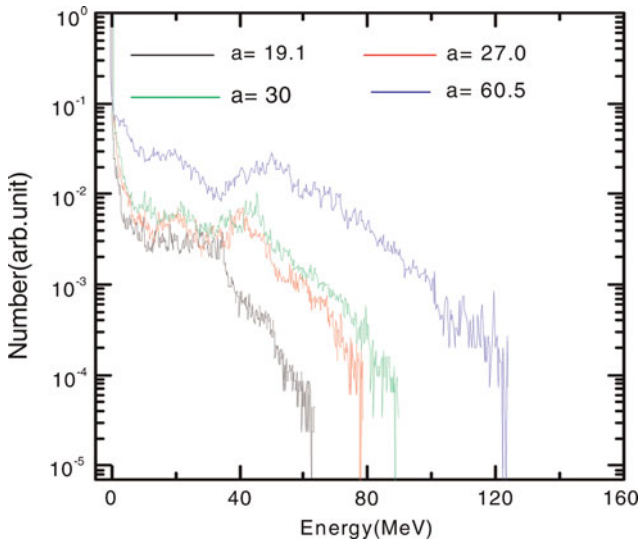

Fig. 5. (Color online) Energy spectra as a function of laser intensity in the 1D-PIC simulations at $t = 500$ laser cycles.

in ion acceleration are qualitatively the same for the two cases.

Figures 7a and b shows the bulk acceleration of deuteron ions along the longitudinal and transverse directions at $t =$ 100 laser cycles, respectively, for normal incidence of the laser pulse. The ions are accelerated inside the foam target in both the forward and backward directions along the longitudinal and transverse directions, respectively. The electric field around each lamellar layer appears to be ambipolar, so the deuterons are accelerated in opposite directions (see Figs.7a and b). The electron return current around these individual layers causes the electric field to be ambipolar. Figure 7c shows the energy distribution of deuteron ions at $t = 100$ laser cycles for both the normal and oblique incidence of the laser pulse. The bulk of the ions are accelerated to maximum energy of 88 MeV. Our 2D-PIC simulations also illustrate that the energy of the ions can be enhanced to approximately 120 MeV with optimized angle of 30° keeping same laser and plasma parameters.

https://doi.org/10.1017/S0263034610000285 Published online by Cambridge University Press

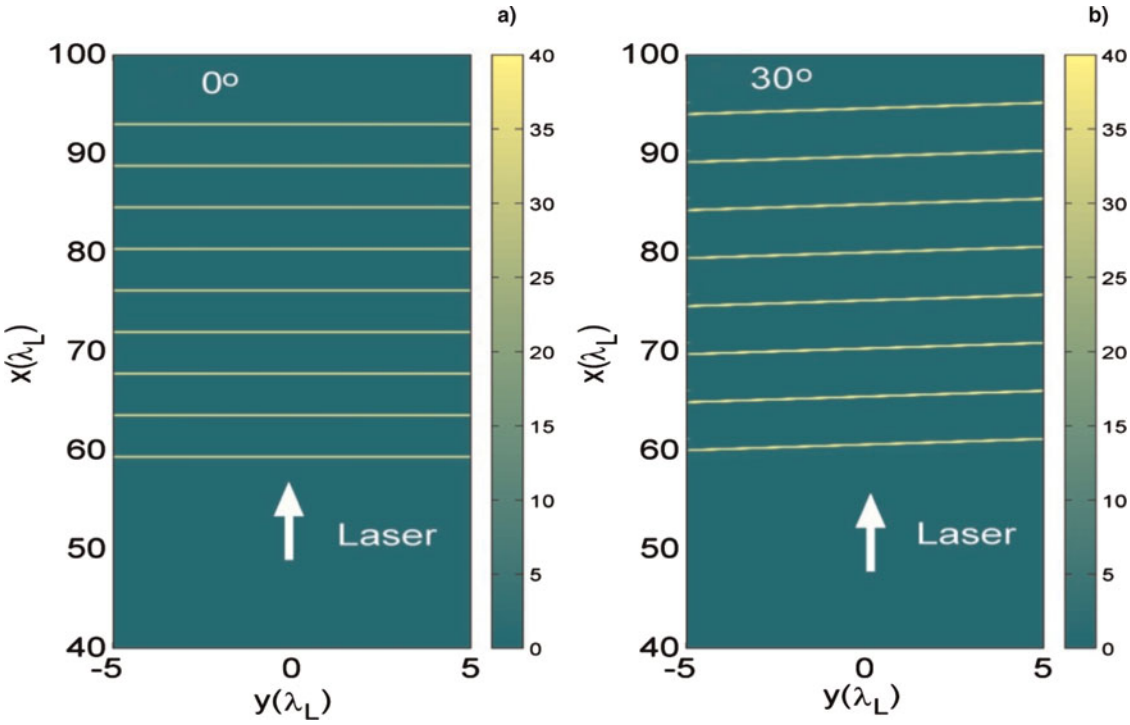

Fig. 6. (Color online) Initial electron density distribution used in the 2D-PIC simulations. (**a**) Normal incidence of the laser pulse on the foam target. (**b**) Oblique incidence of the laser on the foam plasma at an optimized angle of 30°. We simulated the oblique incidence by taking oblique plasma instead of the oblique laser pulse.

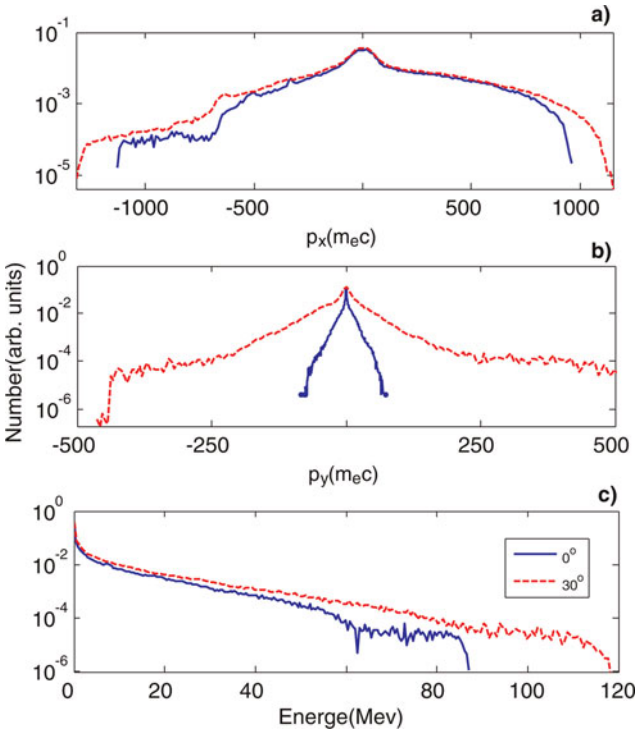

Fig. 7. (Color online) The longitudinal (**a**) and transverse (**b**) momenta of deuteron ions in the 2D-PIC simulation found at $t = 100$ laser cycles for normal and oblique incidence of the laser pulse on the foam target respectively. (**c**) The corresponding energy distributions of deuteron ions at the same time.

CONCLUSIONS

In conclusion, we study deuterium ion acceleration inside a foam target due to the multi-peaked charge separation fields induced around the lamellar layers. We find that the deuterium ions inside the foam target can be accelerated to energies on the order of 88 MeV from foam peak density equal to $40n_c$, separation length($L = 4\lambda_L$) and layer thickness($d = 0.2\lambda_L$), which corresponds to an average density of $2.38n_c$. These foam target parameters are the optimized target parameters for large number of ions with high ion energies.

Finally we observe that laser incidence angle play an important role in defining deuterium ion acceleration from foam target. Deuterons achieve 126 MeV at an optimal angle of 30°. Deuterons inside the foam target are accelerated more effectively in case of oblique incidence due to optimal energy absorption and penetration into the plasma due to conversion of laser pulse energy into nonlinear pulse energy. A detailed experimental understanding of the effect of foam microstructure for ion acceleration is needed.

ACKNOWLEDGMENTS

We thank Prof. S. V. Bulanov for his helpful discussions on this subject. This work is supported in part by the National Natural Science Foundation of China (Grants No. 10674175, 10935002, 10734130), and the National Basic Research Program of China (Grant No. 2007CB815100).

https://doi.org/10.1017/S0263034610000285 Published online by Cambridge University Press

REFERENCES

Andreev, A., Platonov, K. & Kawata, S. (2009). Ion acceleration by short high intensity laser pulse in small target sets. *Laser Part. Beams* **27**, 449–457.

Bagchi, S., Kiran, P.P. & Bhuyan, M.K. (2008). Hotter electrons and ions from nano-structured surfaces. *Laser Part. Beams* **26**, 259–264.

Batani, D., Antonicci, A., Pisani, F., Hall, T.A., Scott, D., Amiranoff, F., Koenig, M., Gremillet, L., Baton, S., Martinolli, E., Rousseaux, C. & Nazarov, W. (2002). Inhibition in the propagation of fast electrons in plastic foams by resistive electric fields. *Phys. Rev. E* **65**, 066409.

Bin, J.H., Lei, A.L., Yang, X.Q., Huang, L.G., Yu, M.Y., Yu, W. & Tanaka, K.A. (2009). Quasi-monoenergetic proton beam generation from a double-layer solid target using an intense circularly polarized laser. *Laser Part. Beams* **27**, 485–490.

Borisenko, N.G., Bugrov, A.E., Burdonskiy, I.N., Fasakhov, I.K., Gavrilov, V.V., Goltsov, A.Y., Gromov, A.I., Khalenkov, A.M., Kovalskii, N.G., Merkuliev, Y.A., Petryakov, V.M., Putilin, M.V., Yankovskii, G.M. & Zhuzhukalo, E.V. (2008). Physical processes in laser interaction with porous low-density materials. *Laser Part. Beams* **26**, 537–543.

Brambrink, E., Roth, M., Blazevic, A. & Schlegel, T. (2006). Modeling of the electrostatic sheath shape on the rear target surface in short-pulse laser-driven proton acceleration. *Laser Part. Beams* **24**, 163–168.

Bulanov, S.V., Naumova, N.M. & Pegoraro, F. (1994). Interaction of an ultrashort relativistically strong laser pulse with an overdense plasma. *Phys. Plasmas* **1**, 745.

Chen, M., Sheng, Z.M., Dong, Q.L., He, M.Q., Li, Y.T., Bari, M.A. & Zhang, J. (2007). Collisionless electrostatic shock generation and ion acceleration by ultraintense laser pulses in overdense plasmas. *Phys. Plasmas* **14**, 053102.

Clark, E.L., Krushelnick, K., Zepf, M., Beg, F.N., Tatarakis, M., Machacek, A., Santala, M.I.K., Watts, I., Norreys, P.A. & Dangor, A.E. (2000). Energetic heavy-ion and proton generation from ultra-intense laser-plasma interactions with solids. *Phys. Rev. Lett*. **85**, 1654.

Eliezer, S., Murakaml, M. & Val, J.M.M. (2007). Equation of state and optimum compression in inertial fusion energy. *Laser Part. Beams* **25**, 585–592.

Fournier, K.B., Constantin, C., Poco, J., Miller, M.C., Back, C.A., Suter, L.J., Satcher, J., Davis, J. & Grun, J. (2004). Efficient multi-KeV X-ray sources from Ti-doped aerogel targets. *Phys. Rev. Lett*. **92**, 165005.

Gibbon, P. & Rosmej, O.N. (2007). Stability of nanostructure targets irradiated by high intensity laser pulses. *Plasma Phys. Contr. Fusion* **49**, 1873–1883.

Hatchett, S.P., Brown, C.G., Cowan, T.E., Henry, E.A., Johnson, J.S., Key, M.H., Koch, J.A., Langdon, A.B., Lasinski, B.F., Lee, R.W., Mackinnon, A.J., Pennington, D.M., Perry, M.D., Phillips, T.W., Roth, M., Sangster, T.C., Singh, M.S., Snavely, R.A., Stoyer, M.A., Wilks, S.C. & Yasuike, K. (2000). Electron, photon, and ion beams from the relativistic interaction of Petawatt laser pulses with solid targets. *Phys. Plasmas* **7**, 2076.

Hoffmann, D.H.H., Blazevic, A., Ni, P., Rosmej, O., Roth, M., Tahir, N.A., Tauschwitz, A., Udrea, S., Varentsov, D., Weyrich, K. & Maron, Y. (2005). Present and future perspectives for high energy density physics with intense heavy ion and laser beams. *Laser Part. Beams* **23**, 47–53.

Hora, H. (2007). New aspects for fusion energy using inertial confinement. *Laser Part. Beams* **25**, 37–45.

Jung, R., Osterholz, J., Löwenbrück, K., Kiselev, S., Pretzler, G., Pukhov, A., Willi, O., Kar, S., Borghesi, M., Nazarov, W., Karsch, S., Clarke, R. & Neely, D. (2005). Study of electron-beam propagation through pre-ionized dense foam plasmas. *Phys. Rev. Letts*. **94**, 195001.

Jungwirth, K. (2005). Recent highlights of the PALS research program. *Laser Part. Beams* **23**, 396–396.

Kulcsár, G., Almawlawi, D., Budnik, F.W., Herman, P.R., Moskovits, M., Zhao, L. & Marjoribanks, R.S. (2000). Intense picosecond X-ray Pulses from laser plasmas by use of nanostructured "velvet" targets. *Phys. Rev. Lett*. **84**, 5149–5152.

Li, Y.T., Sheng, Z.M., Ma, Y.Y., Jin, Z., Zhang, J., Chen, Z.L., Kodama, R., Matsuoka, T., Tamppo, M., Tanaka, K.A., Tsutsumi, T., Yabuuchi, T., Du, K., Zhang, H.Q., Zhang, L. & Tang, Y.J. (2005). Demonstration of bulk acceleration of ions in ultra-intense laser interactions with low-density foams. *Phys. Rev. E* **72**, 066404.

Lifschitz, A.F., Faure, J., Glinec, Y., Malka, V. & Mora, P. (2006). Proposed scheme for compact GeV laser plasma accelerator. *Laser Part. Beams* **24**, 255–259.

Limpouch, J., Psikal, J., Andreev, A.A., Platonov, K.Y. & Kawata, S. (2008). Enhanced laser ion acceleration from mass-limited targets. *Laser Part. Beams*, **26**, 225–34.

Liu, M.P., Xie, B.S., Huang, Y.S., Liu, J. & Yu, M.Y. (2009). Enhanced ion acceleration by collisionless electrostatic shock in thin foils irradiated by ultraintense laser pulse. *Laser Part. Beams* **27**, 327–333.

Mackinnon, A.J., Patel, P.K., Borghesi, M., Clarke, R.C., Freeman, R.R., Habara, H., Hatchett, S.P., Hey, D., Hicks, D.G., Kar, S., Key, M.H., King, J.A., Lancaster, K., Neely, D., Nikkro, A., Norreys, P.A., Notley, M.M., Phillips, T.W., Romagnani, L., Snavely, R.A., Stephens, R.B. & Town, R.P.J. (2006). Proton radiography of a laser-driven implosion. *Phys. Rev. Lett*. **97**, 045001.

Malka, V., Faure, J., Gauduel, Y.A., Lefebvre, E., Rousse, A. & Phuoc, K.T. (2009). Principles and applications of compact laser–plasma accelerators. *Nat. Phys*. **4**, 447.

Morita, T., Esirkepov, T.Zh., Bulanov, S.V., Koga, J. & Yamagiwa, M. (2008). Tunable high-energy ion source via oblique laser pulse incident on a double-layer target. *Phys. Rev. Lett*. **100**, 145001.

Mulser, P., Kanapathipillai, M. & Hoffmann, D.H.H. (2005). Two very efficient nonlinear laser absorption mechanisms in clusters. *Phys Rev Lett*. **95**, 103401.

Naumova, N., Schlegel, T., Tikhonchuk, V.T., Labaune, C., Sokolov, I.V. & Mourou, G. (2009). Hole boring in a DT pellet and fast-ion ignition with ultraintense laser pulses. *Phys. Rev. Lett*. **102**, 025002.

Okihara, S., Esirkepov, T.Zh., Nagai, K., Shmizu, S., Sato, F., Hashida, M., Iida, T., Nishihara, K., Norimatsu, T., Izawa, Y. & Sakabe, S. (2004). Ion generation in a low-density plastic foam by interaction with intense femtosecond laser pulses. *Phys. Rev. E* **69**, 026401.

Patel, P.K., Mackinnon, A.J., Key, M.H., Cowan, T.E., Foord, M.E., Allen, M., Price, D.F., Ruhl, H., Springer, P.T. & Stephens, R. (2003). Isochoric heating of solid-density matter with an ultrafast proton beam. *Phys. Rev. Lett*. **91**, 125004.

Rajeev, P.P., Taneja, P., Ayyub, P., Sandhu, A.S. & Kumar, G.R. (2003). Metal nanoplasmas as bright sources of hard X-ray pulses. *Phys. Rev. Lett*. **90**, 115002.

Ramakrishna, B., Wilson, P.A., Quinn, K., Borghesi, M., Pipahl, A., Willi, O., Lancia, L., Fuchs, J., Clarke, R.J., Notley, M. & Nazarov, W. (2009). Propagation of relativistic electrons in low density foam targets. *Astrophys. & Space. Sci*. **322** 161–165.

Roth, M., Brambrink, E., Audebert, P., Blazevic, A., Clarke, R., Cobble, J., Cowan, T.E., Fernandez, J., Fuchs, J., Geissel, M., Habs, D., Hegelich, M., Karsch, S., Ledingham, K., Neely, D., Ruhl, H., Schlegel, T. & Schreiber, J. (2005). Laser accelerated ions and electron transport in ultra-intense laser matter interaction. *Laser Part. Beams* **23**, 95–100.

Roth, M., Cowan, T.E. Key, M.H., Hatchett, S.P., Brown, C., Fountain, W., Johnson, J., Pennington, D.M., Snavely, R.A., Wilks, S.C., Yasuike, K., Ruhl, H., Pegoraro, F., Bulanov, S.V., Campbell, E.M., Perry, M.D. & Powell, H. (2001). Fast ignition by intense laser-accelerated proton beams. *Phys. Rev. Lett*. **86**, 436–439.

Snavely, R.A., Key, M.H., Hatchett, S.P., Cowan, T.E., Roth, M., Phillips, T.W., Stoyer, M.A., Henry, E.A., Sangster, T.C., Singh, M.S., Wilks, S.C., Mackinnon, A., Offenberger, A., Pennington, D.M., Yasuike, K., Langdon, A.B., Lasinski, B.F., Johnson, J., Perry, M.D. & Campbell, E.M. (2000). Intense High-Energy Proton Beams from Petawatt-Laser Irradiation of Solids. *Phys. Rev. Lett*. **85**, 2945.

Sumeruk, H.A., Kneip, S., Symes, D.R., Churina, I.V., Belolipetski, A.V., Donnelly, T.D. & Ditmire, T. (2007). Control of Strong-Laser-Field Coupling to Electrons in Solid Targets with Wavelength-Scale Spheres. *Phys. Rev. Letts*. **98**, 045001.

Tabak, M., Hammer, J., Glinsky, M.E., Kruer, W.L., Wilks, S.C., Woodworth, J., Campbell, E.M., Perry, M.D. & Mason, R.J. (1994). Ignition and high gain with ultra powerful lasers. *Phys. Plasmas* **1**, 1626.

Temporal, M., Honrubia, J.J. & Atzeni, S. (2002). Numerical study of fast ignition of ablatively imploded deuterium–tritium fusion capsules by ultra-intense proton beams. *Phys. Plasmas* **9**, 3098.

Ter-Avetisyan, S., Schnurer, M., Nickles, P.V., Kalashnikov, M., Risse, E., Sokollik, T., Sandner, W., Tikhonchuk, V.T. & Andreev, A.A. (2006). Quasi monoenergetic deuteron bursts produced by ultra-intense laser pulses. *Phys. Rev. Lett*. **96**, 145006.

Ter-Avetisyan, S., Schnurer, M., Polster, R., Nickles, P.V. & Sandner, W. (2008). First demonstaration of collimation and monochromatisation of a laser accelerated proton burst. *Laser Part Beams* **28**, 637–642.

Wilks, S.C., Langgdon, A.B., Cowan, T.E., Roth, M., Singh, M., Hatchett, S., Key, M.H., Pennington, D., Mackinnon, A. & Snavely, R.A. (2001). Energetic proton generation in ultra-intense laser–solid interactions. *Phys. Plasmas* **8**, 542.

Willingale, L. (2007). Ion acceleration from high intensity laser plasma interactions. PhD thesis. London, UK: Department of Physics Imperial College London.

Winterberg, F. (2008). Lasers for inertial confinement fusion driven by high explosives. *Laser Part. Beams* **26**, 127–135.

Yin, L., Albright, B.J., Hegelich, B.M. & Fernandez, J.C. (2006). GeV laser ion acceleration from ultrathin targets: The laser break-out afterburner. *Phys. Rev. STAB* **24**, 291–298.

Yin, L., Albright, B.J., Hegelich, B.M., Bowers, K.J., Flippo, K.A., Kwan, T.J.T. & Fernandez, J.C. (2007). Monoenergetic and GeV ion acceleration from the laser breakout afterburner using ultrathin targets. *Phys. Plasma* **14**, 056706.

Zhang, J., Li, Y.T., Sheng, Z.M., Ma, Y.Y., Jin, Z., Chen, Z.L., Kodama, R., Matsuoka, T., Tampo, M., Tanaka, K.A., Tsutsumi, T. & Yabuuchi, T. (2005). Bulk acceleration of ions in intense laser interaction with foams. *Plasma Phys. & Contr. Fusion* **47**, B879–B889.